

THERMOGRAPHIC QUALIFICATION OF GRAPHITE/EPOXY INSTRUMENTATION RACKS

James L. Walker¹, Samuel S. Russell² and Gary L. Workman¹

¹University of Alabama in Huntsville
Huntsville, AL 35899
205-890-6578

²National Aeronautics and Space Administration
Marshall Space Flight Center, AL 35812
205-544-4411

ABSTRACT

A nondestructive evaluation method is desired for ensuring the "as manufactured" and "post service" quality of graphite/epoxy instrumentation rack shells. The damage tolerance and geometry of the racks dictate that the evaluation method be capable of identifying defects, as small as 0.25 inch² in area, over large acreage regions, tight compound radii and thickness transition zones. The primary defects of interest include voids, inclusions, delaminations and porosity.

The potential for an infrared thermographic inspection to replace ultrasonic testing for qualifying the racks as "defect free" is under investigation. The inspection process is validated by evaluating defect standard panels built to the same specifications as the racks, except for the insertion of artificially fabricated defects. The artificial defects are designed to closely match those which are most prevalent in the actual instrumentation racks. A target defect area of 0.0625 inch² (a square with 0.25 inch on a side) was chosen for the defect standard panels to ensure the ability to find all defects of the critical (0.25 inch²) size.

Keywords: thermography, graphite/epoxy composites, delamination, porosity

1. INTRODUCTION

One part of the qualification of an aerospace structure for service involves verifying that no defects were created during the manufacturing process and that no damage was produced during handling. This is normally accomplished with a combination of nondestructive evaluation (NDE) methods at various stages of the assembly. The graphite/epoxy instrumentation racks under investigation for this study are qualified through a series of ultrasonic inspections after fabrication. Ultrasonic testing (UT) provides 100 percent coverage of the rack shell and has the potential of locating all critically sized defects. The problem with UT though, is that it is time consuming and requires submersion of the shell in a water tank during the scanning operation. Therefore, the method is not suited for post flight or in-service inspections; i.e. a fully equipped rack. Infrared (IR) thermographic methods on the other hand have proven to be well suited for the inspection of monolithic "shell" structures.

One of the principle advantages of IR thermography over conventional ultrasonic testing is that with thermography large regions are viewed in each inspection operation as opposed to the point by point coverage of UT. Also, no direct contact with the structure is required with thermography, such as the water coupling used with UT, therefore little disassembly of the structure is required. One of the main disadvantages of thermography is that in order for a defect to be detected it must interfere with an externally applied heat pulse in such a way as to develop a change in the normal surface temperature profile. A very tight defect or one that is thermally similar to the surrounding material has little chance of being detected.

The racks under investigation are constructed from an autoclaved graphite/epoxy with 18 ply acreage regions building up to 22 plies in the corners. A protective layer of fiberglass provides the finish layer and serves as a "tattle-tale" for in-service damage. The fiberglass shows as white against the black graphite background when its surface is struck hard enough to produce significant internal damage. The defects of interest include voids, inclusions, delaminations and porosity with a critical area threshold of 0.25 inch².

The work presented in this paper directly addresses qualifying IR thermography to locate porosity, inclusions and delaminations in instrumentation rack shells. The work is divided into two segments. First, the issues of delaminations created by way of impact damage is covered then the ability to locate simulated porosity and inclusions are discussed. The thermographic methods and results from inspection of actual rack panels are also covered.

2. EXPERIMENTAL

2.1 IMPACT DAMAGE ASSESSMENT

Damage created as a result of low energy blunt impacts are particularly troublesome for composite structures, since drastic reductions in strength can be produced even when little or no surface indications are present^{1,2}. The primary type of damage in low energy impacts are delaminations and matrix cracking². Very complex damage patterns can be produced from impact loads and quite often the extent of damage grows in size through the thickness of a sample beneath the impact site. In many cases little or no indication of damage may be present at the impact site while, serious back side and through thickness damage exists³. For this reason it is important to be able to inspect the instrumentation racks, fully loaded and installed as well as between missions.

Selection of the impact energy level was determined by performing a series of tests with different impact tups, drop heights and boundary "panel support" conditions on a section of the instrumentation rack. Table 1 outlines the thirteen impact levels used to determine the correct drop height and Figure 1 shows their locations on the sample rack section. Figure 2 contains the resulting thermograms produced by flash heating the impacted panel. Note that in Figure 2, none of the 9 and 12 inch drop height impacts (impact numbers 5, 6, 9 and 10) produced any detectable thermal indications. These impacts also produced no visual indications and when tested ultrasonically gave no sign of damage. The smallest detectable impact level was produced from a 13.5 inch drop (impact number 3 and 4) using a rubber mat to support the panel at the impact site.

An impact produced by a 0.25 inch tup weighing 2.67 lb, dropped from a height of 13.5 inch (impact number 1), was found to best match the desired defect size and shape. A series of thirty impacts, in a 6 x 5 array, were performed on a section of rack (Table 2) to establish statistically the ability to thermographically locate and evaluate the damage zones. The visible damage area shown in the fiberglass cover ply was measured for reference. The areas ranged from 0.01 to 0.058 inch² on the outer "impact" side of the rack to between 0.015 to 0.078 inch² on the inner surface of the rack panel. In all, only four of the damage areas exceeded the desired defect size limit of 0.0625 inch².

Table 1. Check-out impact loads

Impact	Drop Height (inch)	Tup size (inch)	Support Backing	Outside Area (inch ²)	Inside Area (inch ²)
1	13.5	0.25	No	0.007	0.151
2	13.5	0.25	No	Not visible	0.144
3	13.5	0.25	Yes	0.004	0.040
4	13.5	0.25	Yes	0.031	0.040
5	12	0.25	No	Not visible	Not visible
6	12	0.25	No	Not visible	Not visible
7	15	0.25	No	0.012	0.131
8	15	0.25	No	0.021	0.160
9	9	0.25	No	Not visible	Not visible
10	9	0.25	No	Not visible	Not visible
11	23	0.25	No	0.342	0.650
12	13.5	0.5	No	0.017	0.176
13	21	0.5	No	0.016	0.225

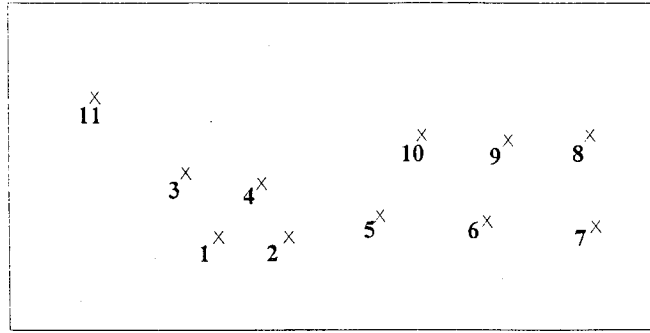


Figure 1. Impact locations for level determination.

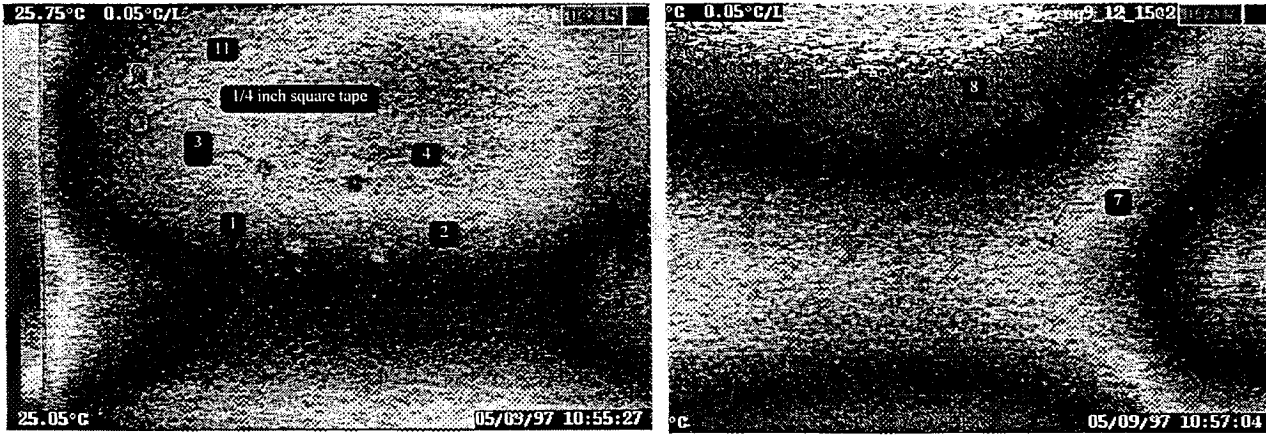


Figure 2. Thermograms of impact damage.

Table 2. Delamination size and impact energies.

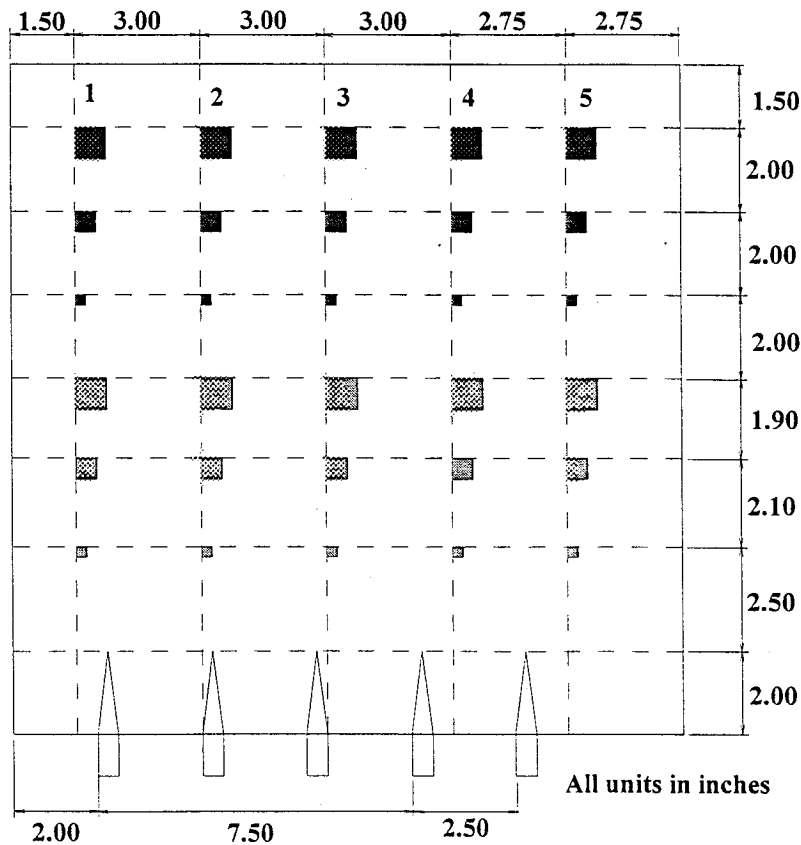
Impact Number	Front Area (in ²)	Rear Area (in ²)	Impact Energy (ft-lbs)
1A	0.031	0.038	5.10
1B	0.038	0.030	4.16
1C	0.043	0.042	5.08
1D	0.057	0.034	5.06
1E	0.043	0.038	5.07
1F	0.047	0.038	4.30
2A	0.011	0.043	5.10
2B	0.044	0.034	5.08
2C	0.037	0.031	5.01
2D	0.036	0.045	5.05
2E	0.013	0.024	4.13
2F	0.058	0.026	5.12
3A	0.016	0.078*	4.94
3B	0.010	0.045	5.07
3C	0.033	0.041	4.25
3D	0.035	0.070*	5.01
3E	0.023	0.042	5.09
3F	0.029	0.039	5.05
4A	0.020	0.038	4.27
4B	0.010	0.026	4.46
4C	0.031	0.070*	5.08
4D	0.040	0.063*	5.04
4E	0.036	0.042	4.27
4F	0.042	0.042	5.06
5A	0.010	0.040	4.40
5B	0.012	0.026	5.06
5C	0.010	0.060	5.11
5D	0.048	0.037	5.07
5E	0.020	0.015	4.59
5F	0.013	0.044	5.05

ROSITY AND INCLUSIONS

manufacture it is possible that regions within the laminate may contain tiny entrapped air bubbles, or porosity. The can come from many sources including; degassing of contaminants (such as oils and silicones); improper debulking air trapped between the plies; or poor ventilation restricting the removal of any degassing of the panel, to name a o matter what the source, porosity can have a detrimental effect on the performance of the structure by leaving of unsupported fibers and points of stress concentration³. If the regions of porosity are large enough they may begin ink under stress and drastically weaken the load carrying capability of the fibers especially when put under sive forces. For the racks under investigation in this paper a 0.25 inch² area of concentrated, or connected, porosity s the critical limit.

to determine the limits of thermographic NDE for detecting porosity two tests were performed. First, a section of a rack own porosity documented through an ultrasonic map was thermographically examined. Second, a 24 ply monolithic el was created with simulated porosity of known size and depth into the laminate. The panel was constructed from onal graphite/epoxy (22 plies) and E-Glass (2 cover plies) similar to that of the actual racks. The simulated defects ed around the critical area by using 0.25, 0.50, 0.75 inch square regions yielding areas of 0.0625, 0.25 and 0.5625 he pattern of planned defects is shown in Figure 3.

at gray regions in Figure 3 depict where the simulated porosity "microballons" (7.0 nm diameter fused silica SiO₂ were placed in the panel. The dark Gray regions in Figure 3 are folded plastic backing material (0.001 inch thick ylene), used to simulate inclusions and disbond areas. Wedge shaped stainless steel shims (0.006 inch thick) were orted into the laminate to create void regions when they were removed after cure and are visible at the bottom of the he defects were placed in five columns so that the depth of inspectability could be investigated. The defects were etween plies (2-3), (5-6), (11-12), (16-17) and (21-22).



. Fabricated test panel.

3. DISCUSSION OF RESULTS

3.1 IMPACT DAMAGE ASSESSMENT

The impacted panel was thermographically inspected using flash heating from the impact side. The coverage area for the imager dictated that the panel be inspected in two passes, each covering an area of the panel 18 inches wide by 12 inches tall. As evident in Figures 4 and 5, all thirty impact locations were identified thermographically. The extent of the damage between impact points as viewed by the thermography system remained fairly constant even though the visual measurements varied greatly between positions (Table 2). The thermograms indicate that the maximum damage area is approximately 0.25 inch square as seen by comparison with the foil tape square in each image. As expected, yet not apparent in the two thermograms shown, the damage appeared to enlarge with depth away from the impact point.

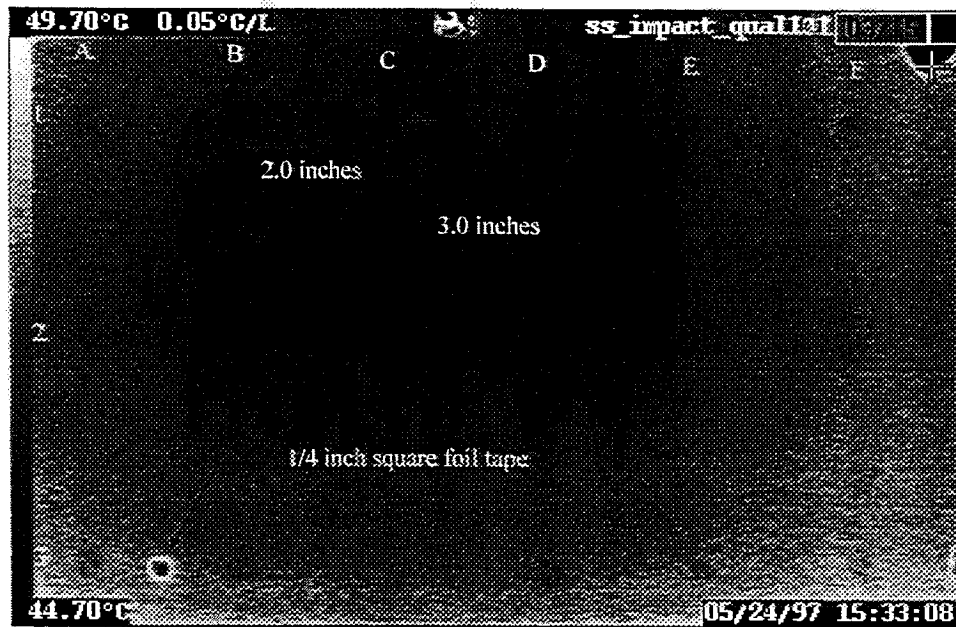


Figure 4. Rows 1, 2 and 3 of qualification impacts.

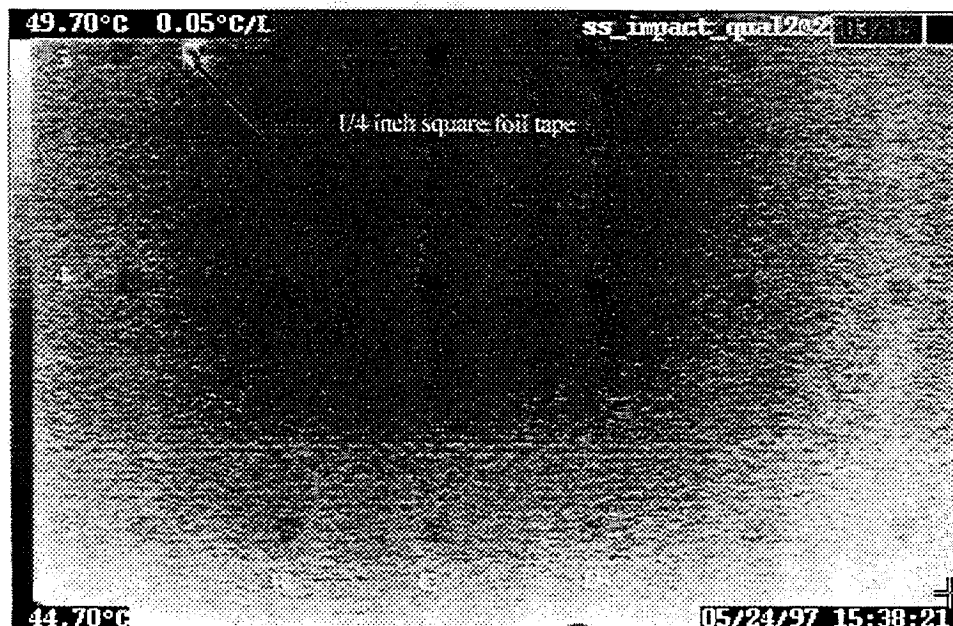


Figure 5. Rows 3, 4 and 5 of qualification impacts.

3.2 POROSITY AND INCLUSIONS

A section of a rack panel with known porosity was inspected thermographically and compared against the UT results. As shown in Figure 6 a close match to the pattern of porosity is given between the UT image and thermogram. In Figure 6 the porosity shows up as a dark patch for the UT image and as a white "hotter" zone on the thermogram. The single thermogram does not show all the details of the UT image since the porosity actually resides throughout the thickness. The UT image measures the complete thickness of the panel while the thermogram shows only the effects from a single slice the cross-section. When several thermograms are viewed over time though, by rastering through the scan history, most if not all of the details in the UT plot can be seen on the thermography image.

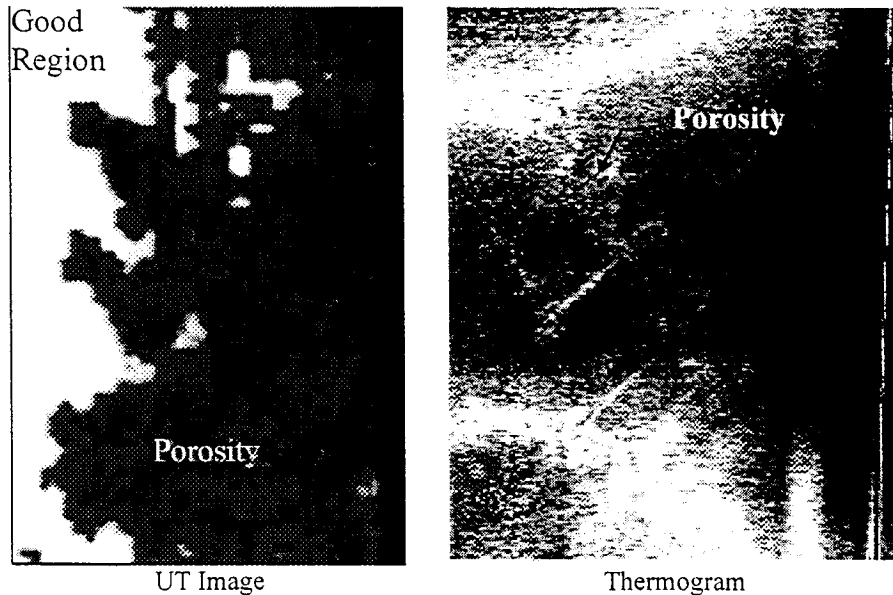


Figure 6. Comparison of Actual Porosity detected by UT and Thermography

In order to verify the depth of penetration of the thermography inspection a specially designed defect panel was constructed (see Section 2.2) and examined. The inspections were accomplished through the use of an Amber Radiance 1 camera with Thermal Wave Imaging software. The imager was positioned sixteen inches from the subject and though the use of a 25 mm lens gave a six inch square field of view. The flash unit used to thermally excite the sampled was set to deliver 1.6 kJ of energy to the surface of the panel.

The resulting thermograms indicate that the limits of the system are somewhere between the second and third column of defects, i.e. between the sixth and eleventh ply. Figure 7 shows the defects from the first column. Those defects in the second column were just barely detectable and did not print well enough to be included in this paper.

The primary drivers behind a successful thermal inspection lies in the ability to get heat into a structure uniformly and with sufficient intensity to create a temporary thermal imbalance around an anomaly as well as to resolve those temperature variations. The structure under test, although appearing to be a good color to absorb heat "black", is somewhat reflective. Due to the high reflectivity, even with a large heat pulse, most of the energy is reflected away from the panel. Possible solutions to this problem included spraying the surface with a flat black water soluble paint, using peal ply during manufacture to dull the surface, or increasing the number of flash heat lamps (input heat energy). Of these solutions, increasing the number of heat lamps would have the least effect on production time but would require doubling the support hardware for the thermographic inspection. Dulling the surface during manufacture with peal ply would not be a likely choice since it would mean reevaluating the structural performance of the rack. The application of a water washable paint appeared to be the best choice for increasing the surface conductivity of the panel.

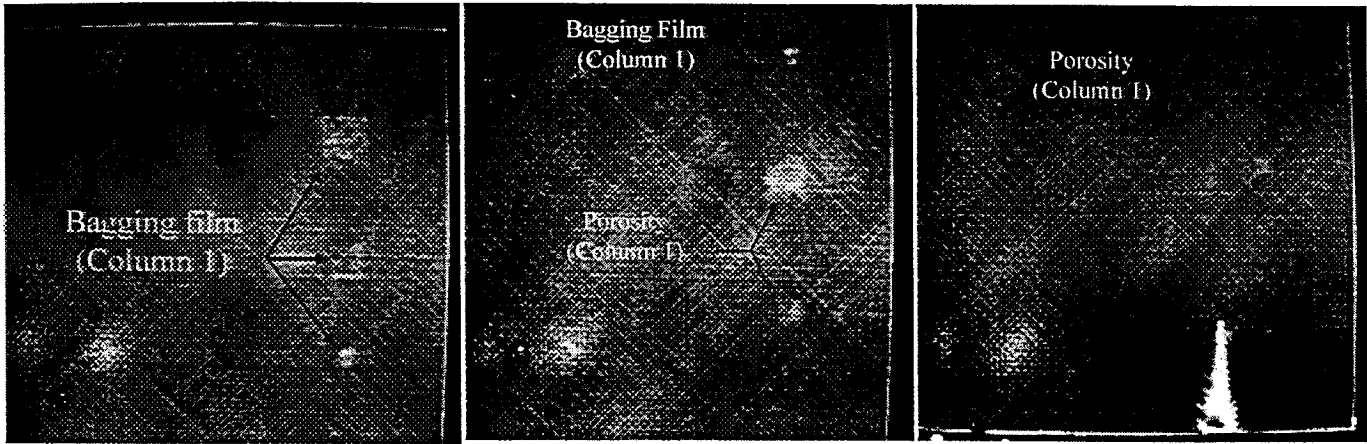


Figure 7. Results from test panel.

As shown in Figure 8, by spraying the surface with a water washable flat black paint it was possible to thermally penetrate to the midply of the laminate. The 0.25 inch square region of porosity is right on the edge of detectability, but can be seen when the thermograms are viewed in a series over time. Although this technique would require that the panel be inspected from both sides and the rack be sprayed and cleaned up after the inspection, it does demonstrate the potential to inspect the racks with thermography.

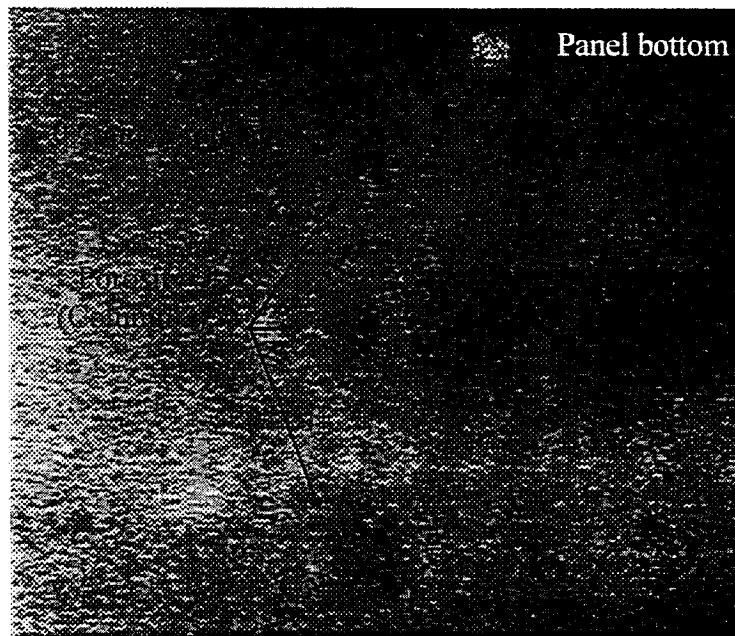


Figure 8. Midply porosity viewed when test panel was painted flat black.

4. CONCLUSIONS

Infrared thermography has been demonstrated to be capable of detecting impact damage “delamination”, porosity and inclusion type defects in the graphite/epoxy instrumentation racks. Good confidence was found for detecting delaminations related to impact damage. The thermographic technique was capable of detecting the subsurface effects of the impact loading that would have been missed with a visual inspection. Porosity close to the surface was found to also be a good

candidate for location with thermography. When the porosity reached depths of six or more plies it is difficult to say with any confidence that it could be detected without some surface preparation of the racks. With the application of a flat black, water washable, paint the porosity at the midplane of the panel was able to be detected. Finally, embedded inclusions and voids were detectable down to about six plies into the laminate and deeper with the addition of a dulling agent to the panels surface.

Additional research will need to be performed to develop methods to raise the sensitivity of the thermographic inspections to a level that will permit one sided inspections without the need for altering the surface finish of the racks. Investigations into image enhancement to increase the sensitivity of the thermographic system, optional heating methods to better excite the defect and finite element methods to determine the theoretical limitations of the system are ongoing.

5. REFERENCES

1. Hill, E. v. K., Walker, J. L. and Rowell, G. H., "Neural Network Burst Pressure Prediction in Graphite/Epoxy Pressure Vessels From Acoustic Emission Amplitude Data," Materials Evaluation Volume 54 Number 6, pp. 744-748, 754, June 1996.
2. Walker, J. L., Russell, S. S., Workman G. L. and Nettles, A., "Impact Damage Characterization of Filament Wound Composite Pressure Vessels," Proceedings from the 1996 ASNT Spring Conference, Norfolk, Virginia, March 18-21, 1996.
3. Hoskin, Brian C. and Baker, Alan A., Composite Materials for Aircraft Structures, AIAA Education Series, pp. 153-174, 1986.